JOURNAL OF BACTERIOLOGY, Feb. 2011, p. 952–962 Vol. 193, No. 4
0021-9193/11/$12.00 doi:10.1128/JB.01161-10


# Pyruvate Formate Lyase Acts as a Formate Supplier for Metabolic Processes during Anaerobiosis in *Staphylococcus aureus*▽

Martina Leibig,[1] Manuel Liebeke,[2]† Diana Mader,[3] Michael Lalk,[2] Andreas Peschel,[3] and Friedrich Götz[1]*

*Interfaculty Institute of Microbiology and Infection Medicine, Microbial Genetics, University of Tübingen, 72076 Tübingen, Germany[1]; Institute for Pharmaceutical Biology, University of Greifswald, 17487 Greifswald, Germany[2]; and Interfaculty Institute of Microbiology and Infection Medicine, Cellular and Molecular Microbiology, University of Tübingen, 72076 Tübingen, Germany[3]*

Received 29 September 2010/Accepted 7 December 2010

**Previous studies demonstrated an upregulation of pyruvate formate lyase (Pfl) and NAD-dependent formate dehydrogenase (Fdh) in *Staphylococcus aureus* biofilms. To investigate their physiological role, we constructed *fdh* and *pfl* deletion mutants (Δ*fdh* and Δ*pfl*). Although formate dehydrogenase activity in the *fdh* mutant was lost, it showed little phenotypic alterations under oxygen-limited conditions. In contrast, the *pfl* mutant displayed pleiotropic effects and revealed the importance of formate production for anabolic metabolism. In the *pfl* mutant, no formate was produced, glucose consumption was delayed, and ethanol production was decreased, whereas acetate and lactate production were unaffected. All metabolic alterations could be restored by addition of formate or complementation of the Δ*pfl* mutant. In compensation reactions, serine and threonine were consumed better by the Δ*pfl* mutant than by the wild type, suggesting that their catabolism contributes to the refilling of formyl-tetrahydrofolate, which acts as a donor of formyl groups in, e.g., purine and protein biosynthesis. This notion was supported by reduced production of formylated peptides by the Δ*pfl* mutant compared to that of the parental strain, as demonstrated by weaker formyl-peptide receptor 1 (FPR1)-mediated activation of leukocytes with the mutant. FPR1 stimulation could also be restored either by addition of formate or by complementation of the mutation. Furthermore, arginine consumption and *arc* operon transcription were increased in the Δ*pfl* mutant. Unlike what occurred with the investigated anaerobic conditions, a biofilm is distinguished by nutrient, oxygen, and pH gradients, and we thus assume that Pfl plays a significant role in the anaerobic layer of a biofilm. Fdh might be critical in (micro)aerobic layers, as formate oxidation is correlated with the generation of $NADH/H^+$, whose regeneration requires respiration.**

*Staphylococcus aureus*, a facultative anaerobic bacterium, is multifaceted during colonization and infection, ranging from an asymptomatic nasal colonizer (17, 47) to an aggressive pathogen that leads to acute infection (18, 49). Many strains may also cause chronic or biofilm-associated infections (23), which are particularly difficult to treat because of increasing multiple antibiotic resistances and high tolerance to the immune defense in a biofilm (24). The tolerance of biofilm-embedded cells to various antibiotics is unclear but can probably be attributed not solely to the exopolysaccharide polysaccharide intercellular adhesin (PIA) (11, 25), which protects the cells; rather, resistance to antibiotics probably results from the altered physiology of biofilm cells. Within a biofilm, cells are exposed to various gradients of nutrients, oxygen, or pH; all of these parameters decrease with the depth of the layers. In comparative expression studies of planktonic and biofilm-grown *S. aureus* cells, it was shown that *pfl*/Pfl (pyruvate formate lyase), *fdh*/Fdh ($NAD^+$-dependent formate dehydrogenase), and *fhs* (formyltetrahydrofolate synthetase) were upregulated at the transcriptional and proteome levels in biofilm (41, 42). It has also been reported that *pfl* is upregulated under anaerobic conditions (20).

The *pfl* gene is found in many bacteria, like *Haemophilus influenzae*, *Clostridium* spp. (27, 48), *Lactobacillus* spp. (1), and *Streptococcus* species (2, 13). However, the enzyme Pfl has been best studied in *Escherichia coli*, where it is involved in mixed-acid fermentation (30, 43, 44). Pfl catalyzes the reversible conversion of pyruvate to formate, thereby producing acetyl coenzyme A (acetyl-CoA) (4), which is important for energy supply when pyruvate is available. The PflB enzyme has to be activated in *E. coli* and related bacteria by a special Pfl activase (PflA) under strict anaerobic conditions (19). This is achieved by forming a glycyl-radical where *S*-adenosylmethionine and reduced flavodoxin serve as cofactors (8).

Soluble Fdh (EC 1.2.1.2) has been reported to occur in methylotrophic bacteria especially (40). In other microorganisms, however, the function has mostly remained unclear thus far. The Fdh enzyme catalyzes the oxidation of formate to carbon dioxide, thereby producing NADH.

Formyl groups, transferred by 10-formyl-tetrahydrofolate (formyl-THF), are important building blocks for a number of key biosynthetic bacterial processes. Bacteria start protein biosynthesis with a formylmethionyl (fMet) start tRNA, with the consequence that all newly synthesized proteins bear an N-terminally formylated methionine. Of note, innate mammalian immune systems can detect formylated peptides very efficiently with their formyl-peptide receptor 1 (FPR1), and the formylated peptides are used as hallmarks for invasive infections,

* Corresponding author. Mailing address: Interfaculty Institute of Microbiology and Infection Medicine, Microbial Genetics, University of Tübingen, 72076 Tübingen, Germany. Phone: (49) 7071 2974636. Fax: (49) 7071 295937. E-mail: friedrich.goetz@uni-tuebingen.de.

† Present address: Biomolecular Medicine, Department of Surgery and Cancer, Faculty of Medicine, Imperial College London, London, United Kingdom SW7 2AZ.

▽ Published ahead of print on 17 December 2010.

TABLE 1. Oligonucleotides used in this study

| Primer | Sequence (5′→3′)[a] | Description |
|---|---|---|
| *fdh* _KO_1F | AAGTCGAATTCCCACAATCACAAATCATCAC | Deletion of *fdh* |
| *fdh* _KO_2R | AATATGGATCCCCCTTGAATTATTGTTAAATTC | Deletion of *fdh* |
| *fdh* _KO_3F | TATTAGTCGACGCTAGCGATTAACGCTTTC | Deletion of *fdh* |
| *fdh* _KO_4R | AATTAGATATCTGATAACGACTTGCATGCCTC | Deletion of *fdh* |
| *fdh* _Kompl_F | ATTTAGGATCCCTTGAAGCAGAGTTGAAGG | Complementation of *fdh* |
| *fdh* _Kompl_R | TTATAGAATTCATTCTATTTAGCTGTATAAC | Complementation of *fdh* |
| *pfl* _KO_1F | TAATAGGTACCCAATTTTACCTTTAAGTATAGG | Deletion of *pfl* |
| *pfl* _KO_2R | ATAATGTCGACCTGTATAATGTTGTGAATTTG | Deletion of *pfl* |
| *pfl* _KO_3F | AATTATCTAGATATTACCATACAAACCATAC | Deletion of *pfl* |
| *pfl* _KO_4R | ATAATAAGCTTACTGCAATAGTAAGGCATTAATG | Deletion of *pfl* |
| *pfl* _Kompl_F | TATTAGGATCCAAAAGTGAATTTTTACGTC | Complementation of *pfl* |
| *pfl* _Kompl_R | TTATAGAATTCGAATTGTATTTATAATTCAAC | Complementation of *pfl* |
| *arcOp* _Kompl_F | TATTACTGCAGGAAAGAATTCATAGTCATTC | Overexpression of *arcOp* |
| *arcOp* _Kompl_R | ATATTGAGCTCATCACCTTAAATTTTACTG | Overexpression of *arcOp* |
| *arcA* _probe_F | TGCGCAGGTGCTAAGAGAAG | Northern blot analysis of *arcA* |
| *arcA* _probe_R | **CTAATACGACTCACTATAGGGAGA**CTGAAACGCCTATAGCCAAG | Northern blot analysis of *arcA* (T7 promoter) |
| *pflB* _probe-F | TGGCGGCATGTGGGATATGG | Northern blot analysis of *pflB* |
| *pflB* _probe-R | **CTAATACGACTCACTATAGGGAGA**TCTGCTGGACGGCTTAAATC | Northern blot analysis of *pflB* (T7 promoter) |

[a] Underlining indicates restriction sites, and boldface indicates the T7 promoter.

since eukaryotic cytoplasmic ribosomes produce only unformylated peptides. FPR1-dependent detection of formylated peptides has major proinflammatory consequences, such as neutrophil influx and degranulation. The source of the formyl groups for the production of formylated proteins and peptides in anaerobically grown bacterial cells has hardly been studied before.

As little is known about Pfl and Fdh in staphylococci, the intention of this study was to investigate the roles of these enzymes under anaerobic conditions and their potential benefit in biofilm. We compared *pfl* and *fdh* deletion mutants with wild-type (wt) cells under various growth conditions. Our findings suggest that Pfl contributes significantly to the supply of formate, which is used via formyl-THF for protein and purine synthesis under anoxic conditions. Fdh most probably plays a role in the microaerobic area of the biofilm, where it contributes to the detoxification of formate and to NADH/$H^+$ production, which can be used as fuel in the respiratory chain. The upregulation of *pfl* and *fdh* thus appears to be an important survival strategy in biofilm.

## MATERIALS AND METHODS

**Bacterial strains and growth conditions.** Primers, strains, and plasmids used in this study are listed with their main characteristics in Tables 1 to 3. All *S. aureus* mutant strains exhibit the SA113 (ATCC 35556) background. Basic medium (BM; 1% soy tryptone, 0.5% yeast extract, 0.5% NaCl, 0.1% $K_2HPO_4$, 0.1% glucose) was used during cloning procedures. If necessary, the medium was supplemented with ampicillin (Am; 100 mg/liter for *E. coli*), chloramphenicol (Cm; 10 mg/liter for *S. aureus*), kanamycin (Km; 30 mg/liter for *E. coli* or 15 mg/liter for *S. aureus*), erythromycin (Em; 2.5 mg/liter for *S. aureus*), or spectinomycin (Spc; 150 mg/liter for *S. aureus*).

For growth studies, bacterial suspensions of overnight cultures were diluted to an optical density at 578 nm ($OD_{578}$) of 0.1. To achieve conditions with decreased oxygen tension, cells were grown in closed Eppendorf tubes (2 ml), with a shaking rate of 150 rpm at 37°C and without addition of antibiotics.

**Construction of the *S. aureus* Δ*pfl* deletion mutant and complementation.** To generate a *pfl* mutant, the plasmid pKO1 (derivative of pBT2 [6; personal communication from B. Krismer]) was used. The *pflB* gene and 249 bp of the *pflA* gene were replaced by the erythromycin resistance cassette *ermB*, derived from pEC3. An upstream flanking region of the target gene (1.1 kb) was amplified by PCR with the primers *pfl* _KO_1F and *pfl* _KO_2R, and a downstream flanking region (1.0 kb) was amplified with the primers *pfl* _KO_3F and *pfl* _KO_4F. The upstream fragment was restricted with Acc65I and SalI and the downstream fragment with XbaI and HindIII. Both fragments were ligated along with the SalI- and XbaI-restricted *ermB* resistance gene (1.5 kb) into pKO1, which was digested with Acc65I and HindIII, respectively. The resulting plasmid, pKO1-*pfl*, was consecutively transferred into *E. coli* XL1-Blue, *S. aureus* strain RN4220, and finally *S. aureus* strain SA113. Allelic replacement of the wild-type *pfl* gene by *erm* in the reverse orientation was carried out as described in the legend of Fig. 1 A. This was confirmed by PCR, restriction digestion, and sequencing.

The Δ*pfl* mutant was complemented by cloning *pflB* and *pflA* under the control of their shared putative promoter into the vector pRB473 (7). The construct was used to consecutively transform *E. coli* XL1-Blue, *S. aureus* RN4220, and finally the deletion mutant *S. aureus* SA113 Δ*pfl* (Fig. 1A).

**Construction of the *S. aureus* Δ*fdh* deletion mutant and complementation.** To replace *fdh*, we used the recently described pBT-*fdh* plasmid (45), a derivate of pBT2, as an allelic-replacement vector. Briefly, a fragment (1.1 kb) of the ho-

TABLE 2. Bacterial strains used in this study

| Strain | Relevant characteristic(s) | Reference |
|---|---|---|
| *E. coli* XL1-Blue | *hsdR17*($r_K^-$ $m_K^+$) *recA1 endA1 gyrA96 thi-1 supE44 relA1 lac* (*F′ proAB lacI*$^q$ZΔM15 Tn*10* [Tet$^r$]) | Stratagene 9 |
| *S. aureus* | | |
| RN4220 | NCTC8325-4 derivative, acceptor of foreign DNA | 26 |
| SA113 (ATCC 35556) | NCTC8325 derivative, *agr* mutant, 11-bp deletion in *rbsU* | 26 |
| SA113 Δ*arcOp* | *arcABDCR*::*lox-72* | 33 |
| SA113 Δ*pfl* | *pflBA′*::*ermB* | This study |
| SA113 Δ*fdh* | *fdh*::*spc* | This study |
| SA113 Δ*pfl* Δ*fdh* | *pflBA′*::*ermB fdh*::*spc* | This study |
| SA113 Δ*pfl* Δ*arcOp* | *pflBA′*::*ermB arcABDCR*::*lox-72* | This study |

TABLE 3. Plasmids used in this study

| Plasmids | Relevant characteristic(s) | Reference |
|---|---|---|
| pBT2 | *cat bla*; *E. coli*/*Staphylococcus* shuttle vector, thermosensitive *ori* for staphylococci | 6 |
| pBT-*fdh* | *cat bla spc*, pBT2 derivative | 45 |
| pKO1-*pfl* | *cat bla ermB*, pBT2 derivative | This study |
| pIC156 | Source of *spc* | 46 |
| pEC3 | Source of *ermB* (from Tn*551*) | 6 |
| pRAB1 | *cat bla* $P_{pagA}$-*cre*, pBT2 derivative | 33 |
| pRB473 | *cat bla ble*; *E. coli*/*Staphylococcus* shuttle vector | 7 |
| pRB-*arcOp* | *cat bla ble arcABDCR*, pRB473 derivative | This study |
| pRB-*pfl* | *cat bla ble pflBA*, pRB473 derivative | This study |
| pRB-*fdh* | SA0170 *cat bla ble fdh*, pRB473 derivative | This study |

mologous upstream region of *fdh* was amplified by PCR using the primers *fdh* _KO_1F and *fdh* _KO_2R, which introduced the restriction sites EcoRI and BamHI, respectively. To provide a homologous downstream sequence, a PCR product of 1 kb generated with the primers *fdh* _KO_3F and *fdh* _KO_4R was restricted with SalI and EcoRV. A spectinomycin resistance cassette (1.3 kb) was obtained from plasmid pIC156 (46) via BamHI/SalI cleavage. The replacement vector was cloned in two steps. First, the downstream fragment was ligated into SalI- and EcoRV-cut pBT2; second, the vector obtained was restricted with SalI and EcoRI, and the upstream and resistant marker fragments were inserted to yield pBT2-*fdh*. The construct was used to transform *S. aureus* RN4220 and *S. aureus* SA113 by electroporation. Allelic replacement of the wild-type *fdh* gene with *spc* in the reverse orientation (Fig. 1B) was carried out as described earlier (6). This was confirmed by PCR, restriction digestion, and sequencing. To complement the *fdh* deletion mutant, the *fdh* gene and the upstream gene encoding a hypothetical protein (SA0170) were cloned together under their own putative promoter into the vector pRB473, resulting in pRB-*fdh*. The construct was used to transform *E. coli* XL1-Blue, *S. aureus* RN4220, and finally the *S. aureus* SA113 Δ*fdh* mutant (Fig. 1B).

**Construction of the *S. aureus* Δ*fdh* Δ*pfl* double mutant.** To generate a *pfl* and *fdh* double mutant, the plasmid pBT2-*pfl* was introduced into the *fdh* deletion mutant. After allelic replacement, the genes *pfl* and *fdh* were replaced by the resistance markers *spc* and *ermB*, respectively.

**Detection of the specific formate dehydrogenase activity.** Quantification was performed as described earlier (42). Briefly, cells were grown aerobically in BM supplemented with 0.67% glucose in flasks (1:8 culture-to-flask volume ratio) at 37°C and 150 rpm. After 24 h, cells were harvested, resuspended in 5 ml of buffer containing 5 mM $MgCl_2$, 1 mM EDTA, and 0.8 M Tris-HCl (pH 7.6), and treated for 15 min with 50 μl lysostaphin (0.5 mg/ml; Sigma) at 37°C. Cells were disrupted three times by vortexing them for 30 s with 200 μg glass beads (diameter, 0.1 mm; Sartorius); in between, the suspensions were kept on ice. After centrifugation (10 min at 15,000 × *g* and 4°C), the supernatant was used for the detection of the formate dehydrogenase. Next, 250 μl of crude cell extract was used, and a buffer containing 10 mM $NAD^+$ and 20 mM formate was added to a final volume of 1 ml. Enzyme activity was detected by an increase of the extinction at 340 nm at room temperature by using the extinction coefficient of NADH ($\varepsilon = 6.3\ mM^{-1}\ cm^{-1}$). Specific activity is expressed as units per mg of protein. Protein concentration was determined by the method of Bradford (5).

**Preparation of crude protein extracts and SDS-PAGE.** Proteins were analyzed by 12% Laemmli SDS-PAGE (32). Samples were grown under decreased oxygen tension in tryptic soy broth (TSB; Sigma) with 0.5% glucose and harvested after 48 h. Cells were adjusted to the same OD and treated with lysostaphin to gain crude cell extracts. Proteins were visualized by staining cells with Coomassie brilliant blue R-250.

**Measurement of glucose, acetate, lactate, and formate in culture supernatants in TSB via enzymatic reactions.** Bacterial suspensions of overnight cultures grown in TSB were diluted and grown under limited-oxygen conditions. After 3 h, 5 h, 8 h, 24 h, and 48 h, samples were taken and the bacteria were spun down. The culture supernatants were treated for 10 min at 80°C, filtered with a sterile filter (0.22 μm), and stored at −20°C until usage. The concentrations of corresponding metabolites were determined with kits purchased from R-Biopharm Inc. according to the manufacturer's instructions, except with the reduction of the reaction batch to 10% to adjust the assays to a microtiter plate scale. All UV assays were based on the increase of NADH or NADPH, which can be monitored spectrophotometrically at a wavelength of 340 nm. Defined dilutions of the metabolites were used to build a calibration curve.

**Analysis of the extracellular metabolome in CDM.** Chemically defined medium (CDM [21]) includes, among other ingredients, alanine, arginine, aspartic acid, cysteine, glutamic acid, histidine, isoleucine, leucine, lysine, phenylalanine, proline, serine, threonine, tryptophan, and valine at a concentration of 1 mM. For growth analysis, overnight cultures were diluted in prewarmed medium and grown under oxygen-limited conditions. The shaking rate was reduced to 100 rpm. Culture supernatants of cells were harvested after 4 h, 6 h, 8 h, 24 h, and 48 h by centrifugation (5 min at 4,500 × *g*) and heating (10 min, 80°C). Subsequently, the solution was filtered with a sterile filter and stored at −20°C. The extracellular metabolome was analyzed with $^1$H nuclear magnetic resonance ($^1$H-NMR), which has recently been described (34). The relative difference was based on (theoretically) added amounts of substances and endpoint quantification (signal intensity relative to that of an internal standard).

**Analysis of the extracellular metabolome and detection of fMet polypeptides in IMDM.** Bacterial cultures grown overnight in tryptic soy broth were used to inoculate lipopolysaccharide (LPS)-free Iscove's modified Dulbecco's medium (IMDM) without phenol red (Gibco) at an $OD_{578}$ of 0.1.

Strains were grown under decreased oxygen tension. When required, 2 mM sodium formate (purissimum pro analysi [p.a.], ≥99.0%; Fluka) was added to the growth medium. For the metabolome analysis, culture supernatants were sampled after 8 h, 24 h, and 48 h, as described for CDM, and analyzed under the same conditions as described above.

Differences in the release of N-terminally formylated peptides were assessed by measuring FPR1-dependent calcium fluxes in human promyelocytic leukemia cells (HL60 cells), which were stably FPR1 transfected (10) upon stimulation with diluted bacterial culture supernatants. To prepare culture supernatants for these measurements, bacterial strains were cultivated either with decreased oxygen tension (as described under "Bacterial strains and growth conditions" above) or aerobically in flasks, with a 1:7 culture-to-flask volume ratio. In some samples, 2 mM sodium formate was added before cultivation. After incubation for 8 or 24 h at 37°C and at 150 rpm, all suspensions were adjusted to an $OD_{578}$ of 1.0. To remove bacteria, suspensions were centrifuged and the culture supernatants were passed through a 0.22-mm-pore-size sterile filter and stored at −20°C. HL60 cells were grown in RPMI 1640 medium supplemented with 10% heat-inactivated fetal calf serum (FCS; Sigma), 20 mM HEPES (Biochrom), 100 mg/ml streptomycin, 100 U/ml penicillin, and 2 mM GlutaMAX (Gibco) as described previously (35). The growth medium of transfected cells was supplemented with 1 mg/ml G418 (Invitrogen). In order to measure calcium ion fluxes, $10^6$ cells/ml were mixed with the calcium-sensitive dye Fluo-3-AM (Molecular Probes) at a final concentration of 2 mM and incubated for 20 min at room temperature in RPMI 1640 medium (Biochrom) supplemented with 0.05% human serum albumin (RPMIeHSA). Subsequently, cells were mixed with diluted staphylococcal culture supernatants at final concentrations of 25% (vol/vol). The corresponding calcium fluxes were monitored after 15 s of incubation in a FACSCalibur flow cytometer (Becton Dickinson) as described recently (15, 35). Untransfected HL60 cells, IMDM, IMDM with 2 mM sodium formate, RPMI 1640 medium, and supernatants of RN4220 Δ*fmt* (data not shown and reference 35) served as negative controls, whereas the synthetic formylated peptide formyl-methionyl-leucyl-phenylalanine (fMLF; 10 nM, final concentration; Sigma) in RPMIeHSA was used as a positive control.

**Construction of the *S. aureus* Δ*pfl* Δ*arcOp* deletion mutant.** To generate a mutant in which the *pfl* gene and the complete *arcABDCR* operon (*arcOp*) were deleted, the plasmid pBT2-*pfl* was introduced into the marker-free *arcOp* deletion mutant described previously (33). Homologous recombination yielded the erythromycin-resistant Δ*pfl* Δ*arcOp* double mutant.

**Cloning of an additional *arcOp*.** To overexpress *arcOp* in *S. aureus* SA113, the entire native *arcABCDR* operon and its putative promoter were amplified by PCR using chromosomal wild-type DNA as a template. The PCR product was cleaved with PstI and SacI and ligated with the similarly restricted pRB473 plasmid.

**Arginine deiminase activity.** The Api Staph assay (28) was used to monitor the arginine deiminase (ADH) activity.

**Growth under an excess of arginine and RNA isolation.** Strains were grown under limited-oxygen conditions in TSB without glucose (1.7% casein peptone [AppliChem], 0.3% soy peptone A3 SC, 0.5% NaCl, 0.25% $K_2HPO_4$; pH 7.2 to 7.4) and in TSB without glucose but supplemented with 20 mM arginine-HCl (pH 7.2 to 7.4); the TSB may, however, contain traces of sugar present in the soy peptone. The absence of glucose is necessary to prevent catabolite repression, as described earlier for *S. aureus* (37).

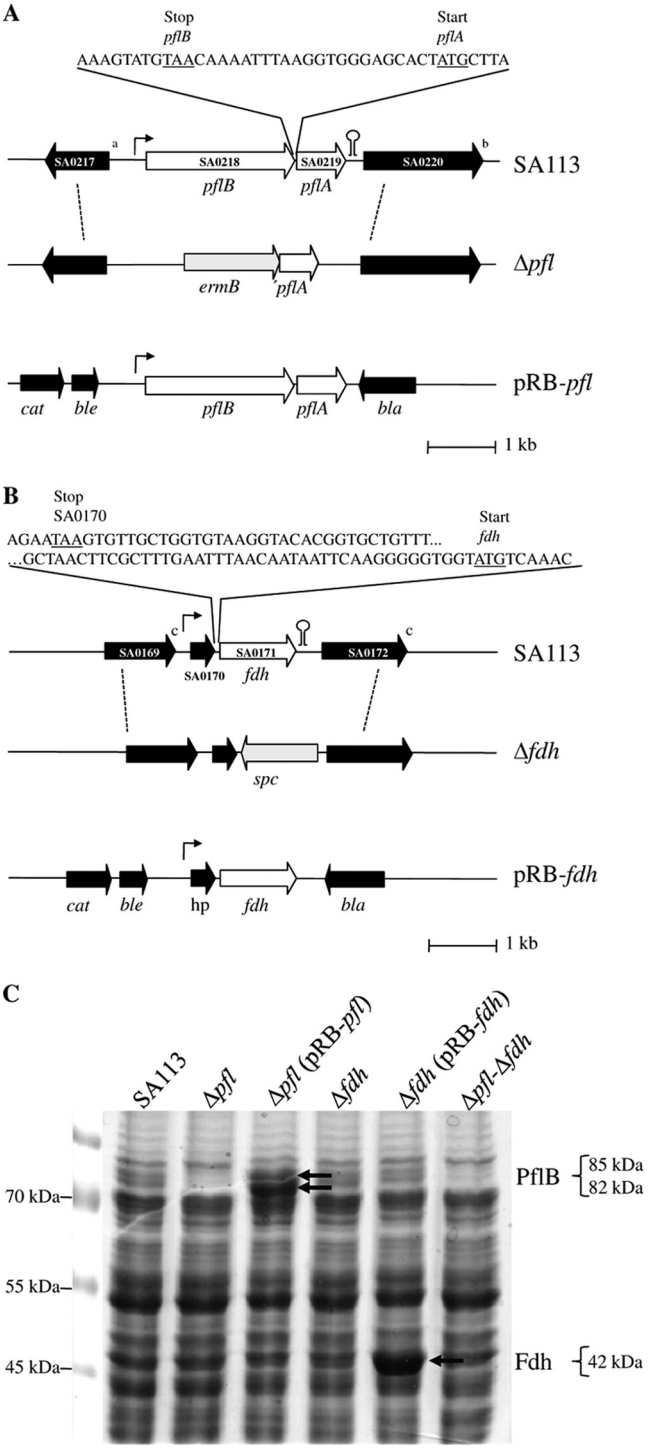


FIG. 1. Scheme of the deletion concept of the pyruvate formate lyase (*pfl*) (A) and formate dehydrogenase (*fdh*) (B). Chromosomal regions of the wild type (upper panels) and the Δ*pfl* and Δ*fdh* deletion mutants (lower panel) are depicted. Dotted lines between the panels indicate the boundaries of homologous regions used for the allelic-replacement vector. Neighboring genes of *pflB* and *pflA* encode the putative iron ABC transporter membrane/binding protein (SA0217) (a) and the putative glycerophosphoryl diester phosphodiesterase (SA0220) (b), and neighboring genes of SA0170/*fdh* encode hypothetical proteins (SA0169 and SA0172) (c). The relevant parts of the complementation plasmids, including the used putative native promoter regions (arrows), are depicted at the bottom. (C) SDS-PAGE analysis of crude extracts, showing relevant molecular masses as indicated by protein markers. Samples derived from SA113, the Δ*pfl* mutant, the Δ*pfl*(pRB-*pfl*) strain, the Δ*fdh* mutant, the Δ*fdh*(pRB-*fdh*) strain, and the Δ*pfl* Δ*fdh* mutant were taken after 48 h of growth in TSB medium with 0.5% glucose under anaerobic conditions. Overexpressed PflB and Fdh are indicated by arrows.

To reach higher cell yields for isolating RNA, cells were grown in 50-ml reaction tubes completely filled with 50 ml TSB without glucose under a shaking rate of 130 rpm at 37°C. The medium, where denoted, was supplemented with arginine. After 4 or 8 h of cultivation, cells were killed by addition of 25 ml of approximately 4°C cold killing buffer (5 mM $MgCl_2$, 20 mM $NaN_3$, 20 mM Tris-HCl [pH 7.5]), harvested by centrifugation (10 min, 4,700 rpm, 4°C), washed, and stored at −70°C until usage. The isolation of total RNA was performed using an acid phenol method with some modifications (22, 36). Cells were disrupted mechanically with 0.5 ml glass beads (diameter, 0.1 mm; Sartorius) in 400 μl phenol-chloroform-isoamyl alcohol (25:24:1) using TissueLyser (Qiagen) for 1 min at 30 Hz. After centrifugation, the upper phase containing the total RNA was extracted with 600 μl phenol-chloroform-isoamyl alcohol (25:24:1) and two times with 600 μl chloroform-isoamyl alcohol (25:1, vol/vol). The RNA was precipitated with 96% ethanol and 3 M Na-acetate. The RNA was resuspended in deionized water. The integrity of the RNA was confirmed by agarose gel electrophoresis.

**Northern blot analysis.** For the Northern blot analysis, an *arcA* RNA probe was prepared by *in vitro* transcription with T7 RNA polymerase using a PCR-generated fragment as the template. Afterward, the probe was labeled with digoxigenin (Roche). The PCR was performed using chromosomal DNA of *S. aureus* SA113 as a template and the primers *arcA* _probe_F and *arcA* _probe_R. By the same procedure, a *pfl* probe was generated using the primers *pflB* _probe-F and *pflB* _probe-R. The 5′ end of the reverse primers represent the T7 promoter. Denaturing 1.5% agarose gels (20 mM MOPS [morpholinepropanesulfonic acid], 5 mM sodium acetate, 1 mM EDTA, 1.85% formaldehyde [pH 7.0]) were used to separate 15 μg (*arcA* mRNA) or 10 μg (*pflB* mRNA) total RNA per well at 120 V in 1× MOPS buffer (20 mM MOPS, 5 mM sodium acetate, 1 mM EDTA [pH 7.0]). After electrophoresis, gels were incubated (5 min) with denaturing buffer (50 mM NaOH, 10 mM NaCl) and neutralized (5 min) with 0.1 M Tris-HCl (pH 7.4). The RNA was transferred to a positively charged nylon membrane with 20× SSPE (3 M NaCl, 0.2 M $NaH_2PO_4$, 20 mM EDTA [pH 7.4]) using a VacuGene XL machine. Blotting of the RNA was fixed to the membrane via UV cross-linking for 1 min. Successful transfer was verified by staining the membrane with methylene blue solution (10% [wt/vol] methylene blue, 0.4 M sodium acetate [pH 5.2], 2% [vol/vol] acetate) to detect the 16S and 23S rRNA bands as a loading control. The digoxigenin-labeled RNA probes were used for gene-specific hybridization according to the manufacturer's instructions (Roche). The hybridization signals were detected using Lumi-Film (Roche).

**Computer sequence analysis.** MacDNASIS Pro v3.5 (Hitachi Software Engineering) as well as Clone Manager 9 (Scientific & Educational Software) were used.

**Statistical analysis.** *P* values were determined using the paired Student *t* test.

## RESULTS

**Construction and characterization of the Δ*pfl* mutant.** In *S. aureus*, *pflB* (SA0218) and *pflA* (SA0219) are oriented in tandem and separated by 23 bp, suggesting that they form an operon that ends with a transcription terminator structure (9.2 kcal) 22 bp downstream of the stop codon of *pflA* (Fig. 1A). Genome annotation of the two genes suggests that PflB (749 amino acids [aa], 85 kDa) represents the proenzyme of Pfl, which can be activated by the introduction of a radical in the catalytic center by the activase PflA (251 aa, 28 kDa) (19).

Genes encoding a putative iron ABC transporter membrane-binding protein (SA0217) as well as a putative two-component sensor histidine kinase (SA0216, not depicted) are located upstream of *pflBA*, separated by 588 nucleotides (nt). Downstream at a distance of 322 bp is a gene encoding

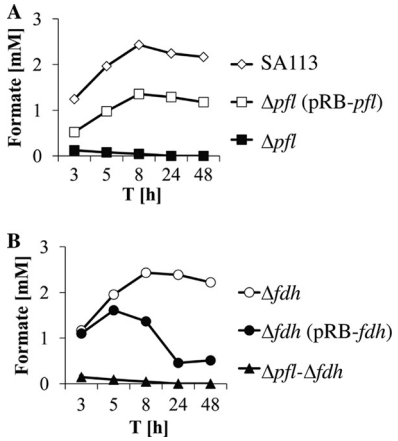


FIG. 2. Formate accumulation in the TSB culture supernatant of anaerobically grown cells. The accumulation of formate was measured in the culture supernatant of SA113, the Δ*pfl* mutant, and the Δ*pfl*-(pRB-*pfl*) strain (A) and in the culture supernatants of the Δ*fdh* mutant, the Δ*fdh*(pRB-*fdh*) strain, and the Δ*pfl* Δ*fdh* mutant (B). The results presented are representative of at least two independent experiments. T, time.

a putative glycerophosphoryl diester phosphodiesterase (SA0220).

In the SA113 Δ*pfl* mutant, *pflB* and part of *pflA* (the first 249 bp of a total of 752 bp) were replaced with the *ermB* (erythromycin resistance gene) cassette as depicted in Fig. 1A. According to the results of SDS-PAGE, the two characteristic protein bands for PflB are absent in the Δ*pfl* mutant but are overexpressed in the pRB-*pfl*-complemented strain (Fig. 1C). The appearance of the double band was first observed in *E. coli* (29) but has also been observed in *S. aureus* (31). When the Pfl of *E. coli*, and probably of *S. aureus*, is radical activated by PflA, exposure to oxygen (during the preparation of the samples) leads to an irreversible cleavage of the enzyme. The 85-kDa band represents the complete Pfl; the 82-kDa band represents the oxygen-inactivated and cleaved form. The Δ*pfl* mutant produced no formate, while the wt excreted up to 2.5 mM formate into the culture supernatant (Fig. 2A). In the pRB-*pfl* (carrying the entire *pflBA* operon)-complemented strain, formate production was mostly restored.

**Construction and characterization of the Δ*fdh* mutant.** The *fdh* gene (SA0171) is followed by a transcription terminator (12.6 kcal) and is flanked by two genes of unknown functions. To construct an *fdh* deletion mutant, the gene was replaced by *spc* (the spectinomycin resistance cassette) (Fig. 1B). In the complementation plasmid pRB-*fdh*, the *fdh* gene was cloned with the upstream SA0170 gene and its promoter-like sequence. The *fdh* gene is most probably transcribed starting from the SA0170 promoter because complementation of the *fdh* mutant was possible only when SA0170 and its upstream region were present.

Under aerobic growth conditions, specific Fdh activity was detectable in the cytoplasmic supernatants of the wt and the complemented mutant but not in supernatant of the Δ*fdh* mutant [SA113, 3.5 ± 2.7 nmol/min/mg protein; Δ*fdh* mutant, no Fdh activity; *fdh*(pRB-*fdh*) strain, 205.3 ± 59.8 nmol/min/mg protein; values represent the averages of results from at least eight independent experiments ± standard deviations].

We expected elevated formate production in the Δ*fdh* mutant under anaerobic conditions because formate, as a Pfl reaction product, cannot be further oxidized to $CO_2$. However, the Δ*fdh* mutant excreted the same amount of formate as the wt in TSB (Fig. 2B). This suggests that the Fdh activity of the wt has little impact on further formate oxidation under anaerobiosis. Only when Fdh was overexpressed in the presence of the complementation plasmid pRB-*fdh* (Fig. 1C) was the formate content in the supernatant significantly decreased (Fig. 2B). No formate was produced in the Δ*pfl* Δ*fdh* (Fig. 2B) and Δ*pfl* Δ*arcOp* (Fig. 7B) double mutants; as shown later, both the transcription of *arcOp* (the arginine deiminase operon) and enzyme activity were enhanced in the Δ*pfl* mutant.

In TSB medium (12.5 mM glucose) under oxygen limitation conditions, no growth differences between the wt, the mutants, and the complemented mutants [the Δ*pfl*, Δ*fdh*, Δ*pfl* Δ*fdh*, Δ*pfl*(pRB-*pfl*), and Δ*fdh*(pRB-*fdh*) strains] could be observed during 48 h of cultivation; the $OD_{578}$ was always in the range of 3.0 (data not shown). All strains produced L- and D-lactate as well as acetate in comparable amounts.

**Addition of formate can largely complement the Δ*pfl* mutant.** Extracellular fermentation products were also determined in IMDM in metabolome studies. IMDM is a highly enriched LPS-free synthetic medium which includes an excess of glucose (25 mM, approximately 2 times more than in TSB). The most obvious differences in fermentation patterns and glucose consumption were observed between the wt and Δ*pfl* strains. In the Δ*pfl* mutant, growth was retarded at 6 and 8 h ($P < 0.001$, $n = 5$) and 10 h ($P < 0.01$, $n = 4$) (SA113 versus the Δ*pfl* mutant), glucose consumption and acidification were markedly delayed, ethanol production was decreased, and, as expected, formate was not produced (Table 4). In the Δ*pfl* (pRB-*pfl*) complemented strain, the wt phenotype was largely restored. A very interesting observation was that the addition of formate (2 mM) to the Δ*pfl* mutant during cultivation also largely restored the wt phenotype. Apparently, the addition of formate has a positive effect on midexponential growth, glucose consumption, and the increase of ethanol production. As shown later, formate serves as a substrate in the biosynthesis of formylated proteins.

**Serine, threonine, and arginine were consumed faster in the Δ*pfl* mutant.** In contrast to IMDM, the CDM that we used contains only 7.5 mM glucose and the added amino acids are present in higher concentrations (1 mM each). Furthermore, CDM does not contain a high content of organic buffer that interferes with $^1$H-NMR measurements. Therefore, CDM is better suited for determining extracellular amino acid consumption by metabolome analysis. Among all the added amino acids, only arginine, serine, and threonine (see Materials and Methods) were consumed more quickly by the Δ*pfl* mutant (Fig. 3). For a control, we also tested the previously described Δ*arcOp* mutant (33), which was unable to consume arginine. Since CDM is very poor in nutrients, growth is limited. The maximum $OD_{578}$s were reached after 10 h, with wt and Δ*fdh* values of 0.6 (24 h/48 h, 0.5), whereas the Δ*pfl* mutant ($OD_{578}$ = 0.7; 24 h/48 h, 0.6) grew slightly better and the Δ*arcOp* mutant ($OD_{578}$ = 0.4; 24 h/48 h, 0.4) somewhat less than the wt. Regarding arginine, serine, and threonine consumption, no difference was found between the wt and the Δ*fdh* mutant, which also held true for the rate of glucose

TABLE 4. Accumulated fermentation products, glucose consumption, pH of culture supernatant, and $OD_{578}$ after anaerobic growth in IMDM[a]

| Parameter | Avg value ± SD at indicated time for: | | | | | | | | | | | |
|---|---|---|---|---|---|---|---|---|---|---|---|---|
| | SA113 | | | Δ*pfl* mutant | | | Δ*pfl*(pRB*pfl*) strain | | | Δ*pfl* mutant + formate[b] | | |
| | 8 h | 24 h | 48 h | 8 h | 24 h | 48 h | 8 h | 24 h | 48 h | 8 h | 24 h | 48 h |
| Lactate production (mM) | 15.0 ± 0.4 | 42.3 ± 2.2 | 44.4 ± 2.6 | 14.8 ± 0.1 | 36.0 ± 4.7 | 47.6 ± 4.3 | 15.3 ± 0.8 | 38.7 ± 1.0 | 40.9 ± 3.0 | 17.7 ± 0.8 | 43.4 ± 0.8 | 46.9 ± 0.8 |
| Ethanol production (mM) | **4.3 ± 0.5** | **10.2 ± 1.1** | **10.5 ± 0.8** | **1.6 ± 0.1** | **3.0 ± 0.1** | **3.2 ± 0.9** | **3.3 ± 0.2** | **9.2 ± 0.4** | **9.8 ± 1.6** | **2.5 ± 0.2** | **7.3 ± 0.2** | **7.4 ± 0.4** |
| Acetate production (mM) | 3.4 ± 0.1 | 2.7 ± 0.2 | 3.6 ± 0.2 | 2.5 ± 0.2 | 2.5 ± 0.1 | 2.6 ± 0.1 | 3.0 ± 0.1 | 2.3 ± 0.1 | 2.6 ± 0.1 | 2.2 ± 0.2 | 1.8 ± 0.0 | 2.2 ± 0.1 |
| Formate production (mM) | **1.9 ± 0.1** | **1.8 ± 0.1** | **1.8 ± 0.1** | **0.0 ± 0.0** | **0.0 ± 0.0** | **0.0 ± 0.0** | **0.9 ± 0.1** | **1.0 ± 0.1** | **1.0 ± 0.1** | **1.4 ± 0.1** | **1.4 ± 0.1** | **1.2 ± 0.1** |
| Succinate production (mM) | 0.2 ± 0.0 | 0.4 ± 0.1 | 0.5 ± 0.0 | 0.1 ± 0.0 | 0.2 ± 0.0 | 0.2 ± 0.0 | 0.2 ± 0.0 | 0.4 ± 0.0 | 0.4 ± 0.1 | 0.2 ± 0.0 | 0.3 ± 0.0 | 0.3 ± 0.0 |
| Glucose consumption (25 mM) | 13.4 ± 0.1 | **0.5 ± 0.4** | 0.0 ± 0.1 | 17.3 ± 1.1 | **7.2 ± 0.6** | 1.2 ± 0.6 | 15.2 ± 1.3 | **2.0 ± 0.5** | 0.0 ± 0.0 | 14.2 ± 1.2 | **2.1 ± 1.2** | 0.0 ± 0.0 |
| pH (7.5) | 6.6 ± 0.1 | **4.6 ± 0.1** | 4.6 ± 0.1 | 6.8 ± 0.1 | **5.9 ± 0.2** | 4.8 ± 0.1 | 6.6 ± 0.0 | **5.0 ± 0.1** | 4.8 ± 0.1 | 6.6 ± 0.0 | **5.1 ± 0.1** | 4.7 ± 0.0 |
| $OD_{578}$ | 1.4 ± 0.1 | 1.3 ± 0.1 | 1.3 ± 0.1 | 1.2 ± 0.1 | 1.7 ± 0.1 | 1.6 ± 0.1 | 1.3 ± 0.2 | 1.6 ± 0.2 | 1.3 ± 0.2 | 1.4 ± 0.1 | 1.8 ± 0.2 | 1.7 ± 0.1 |

[a] Extracellular metabolites, glucose concentration, pH, and optical density were measured after anaerobic growth in IMDM for 8 h, 24 h, and 48 h. Values represent the averages of results from three independent experiments ± standard deviations. The main differences are in boldface.
[b] Two millimolar formate (sodium formate) was added to the growth medium at the beginning of cultivation.

consumption, as well as the rate of formate production and the degradation profile (Fig. 4A and C). Unlike the wt, the Δ*pfl* and Δ*pfl* Δ*fdh* mutants showed no formate accumulation in the culture supernatant (Fig. 4B). In a rich medium, such as TSB and IMDM, formate accumulated in the wt and the Δ*fdh* mutant and stayed at the same level over at least 48 h (Fig. 2 and Table 4). However, in defined and poor media, such as CDM, formate accumulated in the first 8 h and was no longer detectable in the next 24 to 48 h (Fig. 4A). Furthermore, there was no difference with regard to fermentation products due to the low carbon flow through the Pfl (data not shown).

**Growth, pH profile, and *arcABDCR* transcription under an excess amount of arginine.** As shown above, the Δ*pfl* mutant consumes arginine much faster than the wt. To answer the question of whether enhanced arginine catabolism affects growth, we compared the growth rates and pH courses of the wt, the Δ*pfl* mutant, the Δ*arcOp* mutant, and the Δ*pfl* Δ*arcOp* double mutant (Fig. 5A and B). Since *arcOp* is glucose repressed (37), we used TSB without glucose but enriched with 20 mM arginine. Until 24 h, no difference was seen in levels of growth and pHs. A marked difference was observed in the late

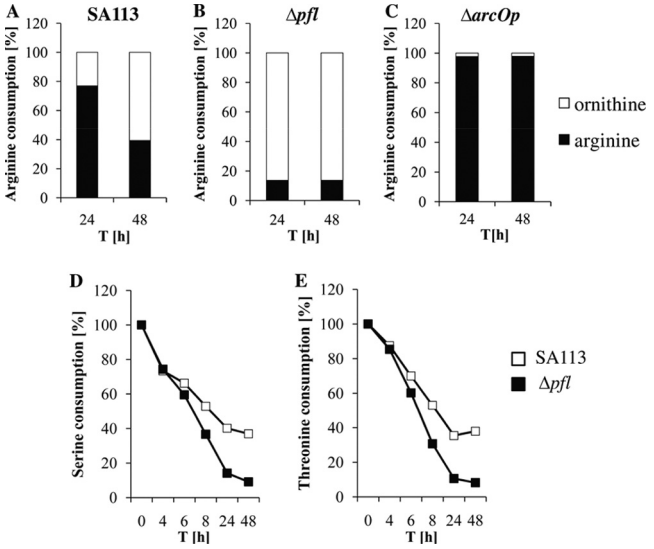


FIG. 3. Differences in the levels of amino acid consumption after anaerobic growth in CDM detected by $^1$H-NMR. In the upper section, the conversion of arginine (black) to ornithine (white) is shown in the culture supernatants of SA113 (A), the Δ*pfl* mutant (B), and the Δ*arcOp* mutant (C). Depicted below are the levels of serine (D) and threonine (E) consumption of SA113 and the Δ*pfl* mutant. The data presented are representative of at least two independent experiments. The initial concentrations of the amino acids (1 mM) were set to 100%.

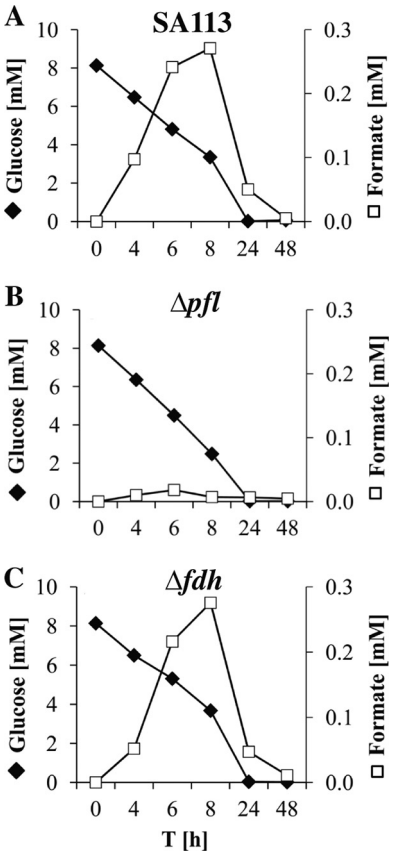


FIG. 4. Glucose consumption (◆) and formate accumulation (□) in culture supernatants as detected by $^1$H-NMR. Samples were taken at the indicated times during growth under oxygen limitation in CDM. The measurements with SA113 (A), the Δ*pfl* mutant (B), and the Δ*fdh* mutant (C) are shown. Absolute values depicted are representative of at least two independent experiments.

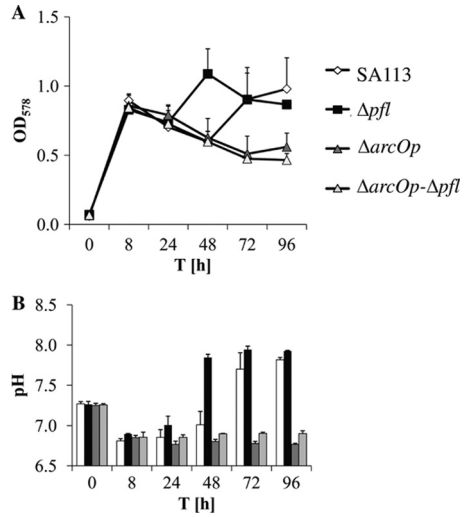


FIG. 5. Microaerobic growth in the presence of arginine. Cells were grown in TSB without glucose but enriched with 20 mM arginine. Optical densities (A) as well as the pH values (B) of SA113 and the Δ*pfl*, Δ*arcOp*, and Δ*pfl* Δ*arcOp* mutants were determined. Bar colors in the bottom panel correspond to the colors used in the key in panel A. Data are expressed as means and standard errors of the means as calculated from at least three biological replicates.

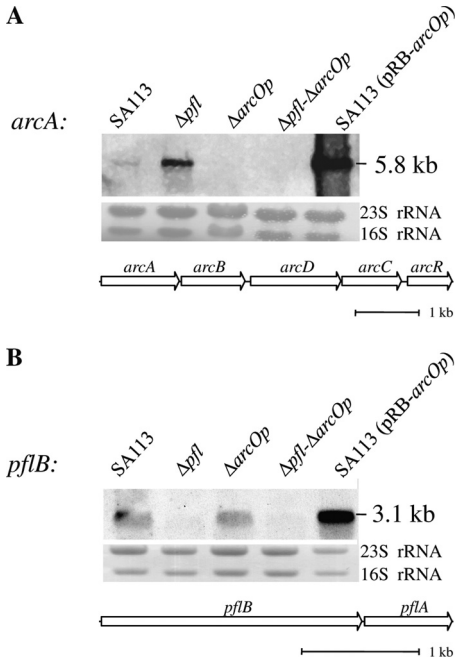


FIG. 6. Northern blot analysis directed against *arcA* (A) and *pflB* (B). Lanes in the upper panels display transcript amounts obtained from SA113, the Δ*pfl* mutant, the Δ*arcOp* mutant, the Δ*pfl* Δ*arcOp* double mutant, and, as a positive control, the wild-type strain harboring the complementation plasmid pRB-*arcOp*. The analyses were conducted with total RNA harvested in the stationary phase (8 h) after growth in the presence of 20 mM arginine. Representative loading controls with 23S and 16S rRNA are shown in the middle panels. Total RNA amounts of 15 μg (A) and 10 μg (B) were loaded per lane. In the lower panels, the schemes of the entire *arc* operon with a size of 5.8 kb (A) or of the *pfl* operon with a size of 3.1 kb (B) are depicted. Images are representative of three independent experiments.

stationary growth phase from 24 to 96 h. After 24 h, the Δ*pfl* mutant started to regrow after a lag phase (diauxie) of approximately 16 h; the wt behaved similarly, but the lag phase was much longer. The regrowth of both strains was correlated with an increase of pH in the medium. Regrowth and alkalization after the lag phase can be explained by the onset of the catabolism of arginine catabolism, which generates ATP and $NH_3$. In contrast to the wt and the Δ*pfl* mutant, the Δ*arcOp* and Δ*pfl* Δ*arcOp* mutants were unable to regrow or to alkalize the medium.

Northern blots were carried out with all strains, and SA113(pRB-*arcOp*) was included as an *arcOp*-overexpressing strain (see Fig. 8A) to test the transcription of *arcOp*. In the Δ*pfl* mutant, the 5,800-nt transcript for *arcOp* was enhanced and was very prominent in the *arcOp*-overexpressing strain. The Δ*arcOp* mutants showed no transcript, as expected. Northern blotting was carried out with cells harvested after 4 and 8 h, as, in later growth phases, RNA degradation was observed.

We also assayed *pfl* transcription in this medium by Northern blotting. As expected, *pfl* was transcribed in the wt and the Δ*arcOp* mutant. No *pflB* expression was detected in the Δ*pfl* mutant and the Δ*pfl* Δ*arcOp* double mutant (Fig. 6B). However, *pfl* transcription was markedly enhanced in the *arcOp*-overexpressing strain SA113(pRB-*arcOp*). We assume that ArcR is a positive regulator both of its own operon and, when overexpressed, of the *pflBA* operon, which is in line with a recent observation that the *pfl* upstream regulatory region carries a Crp-like consensus binding site (37).

**The Δ*pfl* mutant produces less-formylated polypeptides.** To verify the role of Pfl as a formate supplier for biosynthetic pathways depending on one-carbon-unit synthesis (27), the amounts of formylated peptides produced by the wt and mutant strains were compared. The biosynthesis of formylated peptides, purine bases, and other bacterial molecules is dependent on formyl-THF, which can be generated via the oxidation of methylene-THF (serine or glycine utilization) or by formate-THF synthetase (Fhs), ligating THF with formate during ATP consumption. The amount of formylated peptides released by bacterial cells was assessed by measuring responses such as calcium ion fluxes in FPR1-transfected HL60 cells exposed to bacterial culture supernatants (10, 12).

The experiments revealed no differences in the stimulating activities of the culture supernatants of the wt, the Δ*pfl* mutant, and the complemented mutant (pRB-*pfl*) when harvested after 24 h of aerobic growth. This finding is consistent with our expectations, since Pfl is a strictly anaerobic enzyme that is rapidly inactivated when exposed to oxygen. However, after 24 h of anaerobic growth, a 50% decrease in the stimulating capacity of culture supernatants was detected in the Δ*pfl* mutant in comparison to that of wt supernatants (Fig. 7A). Culture supernatants of the Δ*pfl* Δ*arcOp* mutant were included as additional controls and showed the same reduction in calcium mobilization as Δ*pfl* mutant supernatants. Stimulation to the wt level could be restored either by complementation of the Δ*pfl* mutant or by supplementation of the growth medium with 2 mM formate (Fig. 7). Externally added formate did not stimulate the FPR1-transfected HL60 cells or enhance the stimulation level of wt supernatants. These results show the

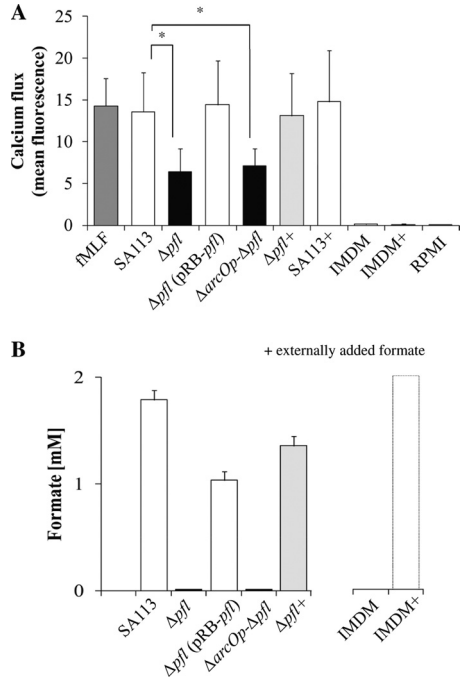


FIG. 7. (A) Calcium flux as a response of HL60 cells stably transfected with FPR1 to culture supernatants of SA113, the Δ*pfl* mutant, the Δ*pfl*(pRB-*pfl*) strain, and, as an additional control, the Δ*arcOp* Δ*pfl* mutant. HL60 cells were incubated with culture supernatants from the indicated *S. aureus* strains grown anaerobically in the absence or presence of formate (indicated by +). Calcium ion fluxes were monitored. fMLF, a synthetic formylated polypeptide, was used as a positive control. Untransfected HL60 cells were completely unresponsive (data not shown). Formate addition *per se* did not affect calcium fluxes in transfected or untransfected HL60 cells. Data represent means of results from at least four independent experiments. *, $P < 0.005$ ($n = 7$). (B) Corresponding formate accumulations in culture supernatants of SA113 strains. Data are expressed as means and standard errors calculated from three biological replicates.

importance of Pfl as a formate supplier for the production of formylated peptides under conditions of anaerobic growth.

## DISCUSSION

In previous studies, it has been shown that under biofilm conditions, genes of formate metabolism, including *pflA* and *pflB* (7-fold) as well as *fdh* (17-fold) and *fhs* (3-fold), were significantly upregulated compared to their expression under conditions of planktonic growth (42). The enhanced transcriptional expression is also reflected at the protein level, where PflB is enhanced 3-fold under biofilm conditions (41). To investigate the benefits of *pfl* and *fdh* in biofilm and in metabolism generally, we generated deletion mutants and compared these mutants with the wild type.

In contrast to the wt, the *fdh* mutant showed no Fdh activity in crude extract, but the mutation had no apparent effect on growth under aerobic and anaerobic conditions. Formate production profiles differed with the medium used. Under anaerobic conditions in rich medium, such as TSB, formate accumulated up to 2.5 mM and remained more or less at this level in both the wt and the *fdh* mutant (Fig. 2A and B). In CDM, there was also no difference between the wt and the *fdh* mutant; however, the accumulated formate was much lower (0.3 mM) and declined after 8 h (Fig. 4). We assume that in nutrient-poor media, the excreted formate is reused for the biosynthesis of formyl-tetrahydrofolate, which is needed for purine and protein synthesis, but that in rich medium, the glucose and amino acid content is much higher, leading to a larger amount of formate. Formate was not produced under aerobic conditions.

First we thought that the *pfl* mutant would accumulate less acetate but more lactate because no acetyl-CoA can be formed and therefore that fermentation could be shifted to lactate. However, in the *pfl* mutant, acetate formation was only marginally affected, ethanol was decreased only 3-fold under glucose excess (IMDM), and formate was not produced at all in any of the media tested. No enhanced lactate production was observed, as described for *pfl* mutants of *E. coli* (50). Another question is how ethanol or acetate is produced in the *pfl* mutant. The most likely candidate is pyruvate dehydrogenase (Pdh), but one cannot rule out the involvement of amino acid metabolism and fatty acid degradation. Normally, Pdh should be active only under aerobic conditions, as its activity is inhibited by high NADH levels. On the other hand, in *Bacillus subtilis*, which lacks *pfl* in its genome, Pdh provides acetyl-CoA also under anaerobic conditions (38).

Exometabolome studies of CDM-grown *S. aureus* indicate that the lack of *pfl* in the mutant can be compensated for by an enhanced utilization of serine, threonine, and arginine. We propose the following assumption, illustrated in Fig. 8A. The catabolic enzymes involved might be the threonine aldolase (SAOUHSC_01307, LtaA [EC 4.1.2.5]) and serine hydroxymethyltransferase (SAOUHSC_02354, GlyA [EC 2.1.2.1]), which are both encoded in the *S. aureus* genome. GlyA, which appears to be essential in *S. aureus* (16), catalyzes the conversion of serine to glycine and thereby provides $C_1$ units via methylene-THF. LtaA converts threonine to glycine and acetaldehyde (not indicated). In both cases, glycine can be further converted via the glycine cleavage system (Gcv) to methylene-THF and finally to formyl-THF. The glycine cleavage system involves the glycine dehydrogenase (SAOUHSC_01632-01633, GcvPB), an aminomethyltransferase T (SAOUHSC_01634, GcvS), and a dihydrolipoamide dehydrogenase (SAOUHSC_01043) (not shown). This putative $C_1$-THF synthesis of the *pfl* mutant is described to occur normally for bacteria under aerobic conditions. The side effects are obvious, since buildup of methylene-THF and formyl-THF from glycine leads to the formation of 1 equivalent of NADH and NADPH. This might be the reason why the wt under anaerobic conditions converts serine to pyruvate via serine-dehydratase (SdaAA). Based on metabolome analysis, the decrease of intracellular serine was correlated with an increase of pyruvate (unpublished data by M. Lalk, University of Greifswald). The formation of NADH causes an adverse NADH/$NAD^+$ ratio, which has been described as being recognized by the Rex regulator, and transcription of the *arc* operon is derepressed (39). In agreement with this theory, arginine consumption is increased (Fig. 3B) and *arc* transcription is also enhanced (Fig. 6A). ATP is thereby produced and might help even by using traces of formate to form formyl-THF. While the *pfl* mutant needs to increase serine and threonine catabolism in order to produce sufficient formyl-THF, in the wt the Pfl produces sufficient

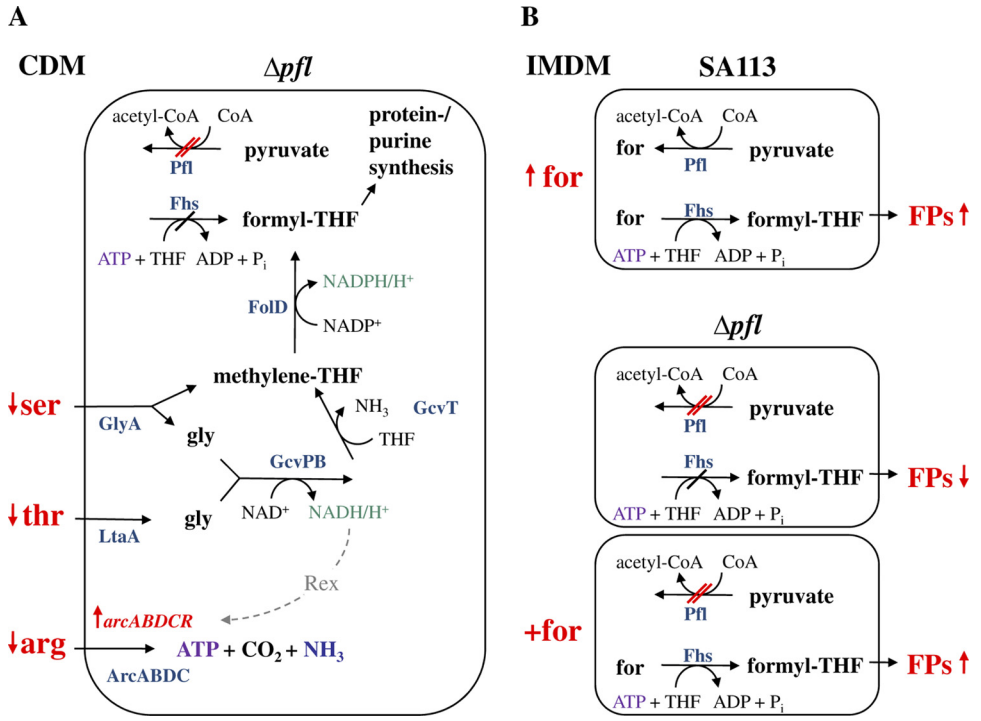


FIG. 8. Schematic hypothesis based on observed metabolic and calcium flux differences (red) in the Δ*pfl* mutant. (A) Differences in the levels of amino acid catabolism observed in CDM. The consumption of serine, threonine, and arginine was enhanced in the Δ*pfl* mutant. The corresponding genes of the putatively involved enzymatic reactions are annotated for *S. aureus* NCTC8325 as follows: for Fhs, a formate-THF ligase (SAOUHSC_01845); GlyA, a serine hydroxymethyltransferase (SAOUHSC_02354); LtaA, a threonine aldolase (SAOUHSC_01307); Gcv, a glycine cleavage system involving the glycine dehydrogenase (SAOUHSC_01632-01633); GcvPB, an aminomethyltransferase T (SAOUHSC_01634); GcvS, a dihydrolipoamide dehydrogenase (SAOUHSC_01043 [not shown]); FolD, a bifunctional protein with methylene-THF dehydrogenase and methenyl-THF cyclohydrolase activity (SAOUHSC_01007); ArcABDCR, an arginine deiminase cluster (SAOUHSC_02969-02964); and Rex, a redox-sensing transcriptional regulator (SAOUHSC_02273). (B) Results detected in glucose-rich IMDM. In contrast to what was obtained with SA113, no formate accumulated in the culture supernatant of the mutant due to the deletion of *pfl* (SAOUHSC_00187-00188). Also, the amount of formylated polypeptides (FPs) was significantly reduced in comparison to amounts in the wt. After addition of formate to the Δ*pfl* mutant, the wt phenotype was restored. ↑for, increased accumulation of formate; +for, added formate.

formate to directly produce formyl-THF via Fhs. The anabolic function of Pfl in building up $C_1$ units for formyl-THF biosynthesis was first described for *Clostridium kluyveri* (27). In *E. coli*, Pfl appears to be used preferentially in catabolism, as *E. coli* does not possess Fhs activity (14).

We also asked whether formate represents the formyl-group donor for the biosynthesis of fMet polypeptides under anaerobic conditions, which depends on the formylation of the start methionyl tRNA by formyl-THF in all bacteria. As the amounts of formyl-THF can hardly be monitored by common analytical methods, we quantified the end products, formylated peptides, by a sensitive bioassay. This assay is based on the observation that formylated peptides lead to intracellular accumulation of $Ca^{2+}$ in human leukocytes at picomolar concentrations via the FPR1 receptor. Formate cannot be generated directly from glucose, as in the wild type, but it is most probably generated from amino acids in the *pfl* mutant. Indeed, we found that stimulatory capacity decreased by 50% in *pfl* mutant supernatants compared to that in wild-type supernatants (Fig. 7A and 8B), which could be restored by supplementation of the growth medium with formate, indicating the importance of formate as a prerequisite for the production of a normal level of formylated peptides. In this context, it would be interesting to know whether formate also leads to the formylation of Pdh and whether formylation affects Pdh activity. We assume that Pdh activity is positively affected by formylation, because when formate was added to the Δ*pfl* mutant, the ethanol production was also enhanced almost to the wt level (Table 5). Furthermore, in a proteome analysis with *Bacillus subtilis*, it has been shown that in at least one enzyme of the Pdh, PdhD, the formyl group was retained (3).

The reason to study the physiological roles of *fdh* and *pfl* in more detail goes back to the previous observation that both genes were significantly upregulated under biofilm conditions compared to under conditions of planktonic growth. Most of our studies were carried out under planktonic conditions, but we also studied biofilms formed on a dialysis membrane. However, the problems with the latter approach were that the biofilm cells were extremely sticky and hard to separate and that in CDM medium anaerobic growth was very weak and almost no biofilm was formed. Therefore, biofilm-related survival or metabolome studies were technically hardly feasible. However, we anticipate that the results obtained with liquid medium can be transferred to the biofilm situation, as shown in Fig. 9. According to this model, upregulation of *pfl* takes place in the deeper layer of the biofilm, where anoxic conditions are prevalent (Pfl is oxygen sensitive) and nutrients are limited. Under these conditions, Pfl is necessary, as it allows the for-

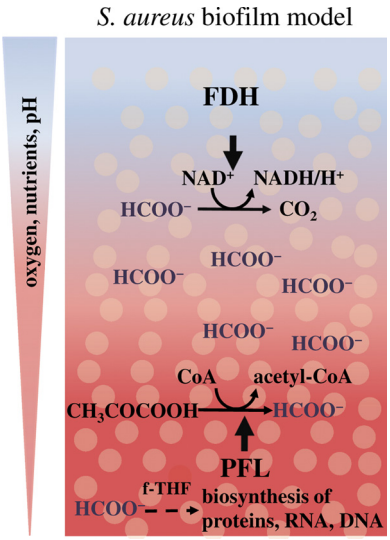


FIG. 9. Schematic representation of formate metabolism in *S. aureus* biofilms. In the anaerobic layers (red) of the mature biofilm, the PFL converts pyruvate to acetyl-CoA and formate. The latter can be used by strictly anaerobically grown cells for the synthesis of formyl-THF and therefore for the biosynthesis of proteins, DNA, and RNA. At the same time, formate accumulates and diffuses to microaerobic regions (light red). Here, it might be oxidized by the FDH under the production of NADH.

mation of $C_1$ units (formate) for formyl-THF synthesis and, consequently, for protein and purine biosynthesis. Interestingly, not only *fdh* and *pfl*, but also the formyl-THF synthetase gene (*fhs*), were upregulated under biofilm growth (42). We found no conspicuous phenotype of the *fdh* mutant under anaerobic or aerobic planktonic conditions (data not shown). Therefore, we suggest that the observed upregulation of *fdh* is biofilm specific, which is also in line with a 7.5-fold-enhanced Fdh activity in biofilm-grown cells (42). Our hypothesis is that Fdh plays a role in the microaerobic area of the biofilm. Formate is produced in the anaerobic area by Pfl and diffuses to the microaerobic region, where it is oxidized by Fdh to produce $CO_2$ and $NADH/H^+$. This has two advantages: first, formate is detoxified, and second, in the presence of small amounts of oxygen, $NADH/H^+$ can be respired and no longer comprises a burden for *S. aureus*. The importance of Pfl under anoxic conditions lies in its ability to supply the cells with sufficient formate, which is used via formyl-THF for protein and purine synthesis. The consequence is that in the *pfl* mutant, much less fMet-polypeptides were produced than in the wt. Because of the mentioned benefits of functional *pfl*, *fdh*, and *fhs*, we conclude that the upregulation of these genes might be an important survival strategy in biofilm.

## ACKNOWLEDGMENTS

We thank Bernhard Krismer for providing the plasmid pKO1 and discussion, Melanie Kull for advice and discussion, and Ralf Rosenstein for critical reading of the manuscript. For technical assistance, we thank Nele Nikola, Detlinde Futter-Bryniok, and Anne Winter.

This work was supported by the funding networks of the German Research Council (grant SFB-TR34 to F. Götz, A. Peschel, and M. Leibig and grant SFB685 to A. Peschel). M. Liebeke was a recipient of a fellowship from the Alfried Krupp von Bohlen and Halbach-Stiftung (Functional Genomics Approach in Infection Biology).

## REFERENCES

1. **Arnau, J., F. Jorgensen, S. M. Madsen, A. Vrang, and H. Israelsen.** 1997. Cloning, expression, and characterization of the *Lactococcus lactis pfl* gene, encoding pyruvate formate-lyase. J. Bacteriol. **179:**5884–5891.
2. **Asanuma, N., and T. Hino.** 2000. Effects of pH and energy supply on activity and amount of pyruvate formate-lyase in *Streptococcus bovis*. Appl. Environ. Microbiol. **66:**3773–3777.
3. **Bandow, J., et al.** 2003. The role of peptide deformylase in protein biosynthesis: a proteomic study. Proteomics **3:**299–306.
4. **Becker, A., et al.** 1999. Structure and mechanism of the glycyl radical enzyme pyruvate formate-lyase. Nat. Struct. Biol. **6:**969–975.
5. **Bradford, M. M.** 1976. A rapid and sensitive method for the quantitation of microgram quantities of protein utilizing the principle of protein-dye binding. Anal. Biochem. **72:**248–254.
6. **Brückner, R.** 1997. Gene replacement in *Staphylococcus carnosus* and *Staphylococcus xylosus*. FEMS Microbiol. Lett. **151:**1–8.
7. **Brückner, R.** 1992. A series of shuttle vectors for *Bacillus subtilis* and *Escherichia coli*. Gene **122:**187–192.
8. **Buis, J., and J. Broderick.** 2005. Pyruvate formate-lyase activating enzyme: elucidation of a novel mechanism for glycyl radical formation. Arch. Biochem. Biophys. **433:**288–296.
9. **Bullock, W. O., J. M. Fernandez, and J. M. Short.** 1987. XL1-Blue: a high efficiency plasmid transforming *recA Escherichia coli* strain with beta-galactosidase selection. Biotechniques **5:**376–382.
10. **Christophe, T., et al.** 2001. The synthetic peptide Trp-Lys-Tyr-Met-Val-Met-NH2 specifically activates neutrophils through FPRL1/lipoxin A4 receptors and is an agonist for the orphan monocyte-expressed chemoattractant receptor FPRL2. J. Biol. Chem. **276:**21585–21593.
11. **Cramton, S. E., C. Gerke, N. F. Schnell, W. W. Nichols, and F. Götz.** 1999. The intercellular adhesion (*ica*) locus is present in *Staphylococcus aureus* and is required for biofilm formation. Infect. Immun. **67:**5427–5433.
12. **Dahlgren, C., et al.** 2000. The synthetic chemoattractant Trp-Lys-Tyr-Met-Val-DMet activates neutrophils preferentially through the lipoxin A(4) receptor. Blood **95:**1810–1818.
13. **Derzelle, S., A. Bolotin, M. Y. Mistou, and F. Rul.** 2005. Proteome analysis of *Streptococcus thermophilus* grown in milk reveals pyruvate formate-lyase as the major upregulated protein. Appl. Environ. Microbiol. **71:**8597–8605.
14. **Dev, I. K., and R. J. Harvey.** 1982. Sources of one-carbon units in the folate pathway of *Escherichia coli*. J. Biol. Chem. **257:**1980–1986.
15. **Dürr, M. C., et al.** 2006. Neutrophil chemotaxis by pathogen-associated molecular patterns—formylated peptides are crucial but not the sole neutrophil attractants produced by *Staphylococcus aureus*. Cell. Microbiol. **8:**207–217.
16. **Forsyth, R. A., et al.** 2002. A genome-wide strategy for the identification of essential genes in *Staphylococcus aureus*. Mol. Microbiol. **43:**1387–1400.
17. **Foster, T. J.** 2004. Nasal colonization by *Staphylococcus aureus*. Nat. Med. **10:**447. (Letter.)
18. **Foster, T. J.** 2004. The *Staphylococcus aureus* "superbug." J. Clin. Invest. **114:**1693–1696.
19. **Frey, M., M. Rothe, A. F. Wagner, and J. Knappe.** 1994. Adenosylmethionine-dependent synthesis of the glycyl radical in pyruvate formate-lyase by abstraction of the glycine C-2 pro-S hydrogen atom. Studies of [2H]glycine-substituted enzyme and peptides homologous to the glycine 734 site. J. Biol. Chem. **269:**12432–12437.
20. **Fuchs, S., J. Pane-Farre, C. Kohler, M. Hecker, and S. Engelmann.** 2007. Anaerobic gene expression in *Staphylococcus aureus*. J. Bacteriol. **189:**4275.
21. **Gaupp, R., S. Schlag, M. Liebeke, M. Lalk, and F. Götz.** 2010. Advantage of up-regulation of succinate dehydrogenase in *Staphylococcus aureus* biofilm. J. Bacteriol. **192:**2385–2394.
22. **Gertz, S., et al.** 1999. Regulation of B-dependent transcription of *sigB* and *asp23* in two different *Staphylococcus aureus* strains. Mol. Gen. Genet. **261:**558–566.
23. **Götz, F.** 2002. *Staphylococcus* and biofilms. Mol. Microbiol. **43:**1367–1378.
24. **Hall-Stoodley, L., and P. Stoodley.** 2009. Evolving concepts in biofilm infections. Cell. Microbiol. **11:**1034–1043.
25. **Heilmann, C., et al.** 1996. Molecular basis of intercellular adhesion in the biofilm-forming *Staphylococcus epidermidis*. Mol. Microbiol. **20:**1083–1091.
26. **Iordanescu, S., and M. Surdeanu.** 1976. Two restriction and modification systems in *Staphylococcus aureus* NCTC8325. J. Gen. Microbiol. **96:**277–281.
27. **Jungermann, K. A., W. Schmidt, F. H. Kirchniawy, E. H. Rupprecht, and R. K. Thauer.** 1970. Glycine formation via threonine and serine aldolase. Its interrelation with the pyruvate formate lyase pathway of one-carbon unit synthesis in *Clostridium kluyveri.* Eur. J. Biochem. **16:**424–429.
28. **Kloos, W. E., and J. F. Wolfshohl.** 1982. Identification of *Staphylococcus* species with the API STAPH-IDENT system. J. Clin. Microbiol. **16:**509–516.
29. **Knappe, J., H. P. Blaschkowski, P. Grobner, and T. Schmitt.** 1974. Pyruvate formate-lyase of *Escherichia coli*: the acetyl-enzyme intermediate. Eur. J. Biochem. **50:**253–263.
30. **Knappe, J., and G. Sawers.** 1990. A radical-chemical route to acetyl-CoA: the anaerobically induced pyruvate formate-lyase system of *Escherichia coli*. FEMS Microbiol. Rev. **6:**383–398.

31. **Kohler, C., et al.** 2003. Physiological characterization of a heme-deficient mutant of *Staphylococcus aureus* by a proteomic approach. J. Bacteriol. **185:**6928–6937.
32. **Laemmli, U. K.** 1970. Cleavage of structural proteins during the assembly of the head of bacteriophage T4. Nature **227:**680–685.
33. **Leibig, M., et al.** 2008. Marker removal in staphylococci via Cre recombinase and different *lox* sites. Appl. Environ. Microbiol. **74:**1316–1323.
34. **Liebeke, M., V. S. Brozel, M. Hecker, and M. Lalk.** 2009. Chemical characterization of soil extract as growth media for the ecophysiological study of bacteria. Appl. Microbiol. Biotechnol. **83:**161–173.
35. **Mader, D., M. J. Rabiet, F. Boulay, and A. Peschel.** 2010. Formyl peptide receptor-mediated proinflammatory consequences of peptide deformylase inhibition in *Staphylococcus aureus*. Microbes Infect. **12:**415–419.
36. **Majumdar, D., Y. J. Avissar, and J. H. Wyche.** 1991. Simultaneous and rapid isolation of bacterial and eukaryotic DNA and RNA: a new approach for isolating DNA. Biotechniques **11:**94–101.
37. **Makhlin, J., et al.** 2007. *Staphylococcus aureus* ArcR controls expression of the arginine deiminase operon. J. Bacteriol. **189:**5976–5986.
38. **Nakano, M., Y. Dailly, P. Zuber, and D. Clark.** 1997. Characterization of anaerobic fermentative growth of *Bacillus subtilis*: identification of fermentation end products and genes required for growth. J. Bacteriol. **179:**6749–6755.
39. **Pagels, M., et al.** 2010. Redox sensing by a Rex-family repressor is involved in the regulation of anaerobic gene expression in *Staphylococcus aureus*. Mol. Microbiol. **76:**1142–1161.
40. **Popov, V. O., and V. S. Lamzin.** 1994. NAD(+)-dependent formate dehydrogenase. Biochem. J. **301:**625–643.
41. **Resch, A., et al.** 2006. Comparative proteome analysis of *Staphylococcus aureus* biofilm and planktonic cells and correlation with transcriptome profiling. Proteomics **6:**1867–1877.
42. **Resch, A., R. Rosenstein, C. Nerz, and F. Götz.** 2005. Differential gene expression profiling of *Staphylococcus aureus* cultivated under biofilm and planktonic conditions. Appl. Environ. Microbiol. **71:**2663–2676.
43. **Sawers, G., and G. Watson.** 1998. A glycyl radical solution: oxygen-dependent interconversion of pyruvate formate-lyase. Mol. Microbiol. **29:**945–954.
44. **Sawers, R. G.** 2005. Formate and its role in hydrogen production in *Escherichia coli*. Biochem. Soc. Trans. **33:**42–46.
45. **Stary, E., et al.** 2010. New architectures for Tet-on and Tet-off regulation in *Staphylococcus aureus*. Appl. Environ. Microbiol. **76:**680–687.
46. **Steinmetz, M., and R. Richter.** 1994. Easy cloning of mini-Tn*10* insertions from the *Bacillus subtilis* chromosome. J. Bacteriol. **176:**1761–1763.
47. **Weidenmaier, C., et al.** 2004. Role of teichoic acids in *Staphylococcus aureus* nasal colonization, a major risk factor in nosocomial infections. Nat. Med. **10:**243–245.
48. **Weidner, G., and G. Sawers.** 1996. Molecular characterization of the genes encoding pyruvate formate-lyase and its activating enzyme of *Clostridium pasteurianum*. J. Bacteriol. **178:**2440–2444.
49. **Young, L. M., and C. S. Price.** 2008. Community-acquired methicillin-resistant *Staphylococcus aureus* emerging as an important cause of necrotizing fasciitis. Surg. Infect. (Larchmt.) **9:**469–474.
50. **Zhu, J., and K. Shimizu.** 2004. The effect of *pfl* gene knockout on the metabolism for optically pure D-lactate production by *Escherichia coli*. Appl. Microbiol. Biotechnol. **64:**367–375.